

# Low temperature coefficient of resistivity induced by magnetic transition and lattice contraction in $\text{Mn}_3\text{NiN}$ compound

Ying Sun,<sup>a</sup> Cong Wang,<sup>a,\*</sup> Lihua Chu,<sup>a</sup> Yongchun Wen,<sup>a</sup> Man Nie<sup>a</sup> and Fusheng Liu<sup>b</sup>

<sup>a</sup>Center for Condensed Matter and Materials Physics, School of Physics, Beihang University, Beijing 100083, China

<sup>b</sup>College of Materials Science and Engineering, Shenzhen University, Shenzhen 518060, China

Received 27 December 2009; revised 12 January 2010; accepted 13 January 2010

Available online 18 January 2010

We report the low temperature coefficient of resistivity (TCR) of antiperovskite  $\text{Mn}_3\text{NiN}$  compound for the first time. Interestingly, the resistivity remained almost constant with temperature from 250 K. The  $d\rho/dT$  value and the TCR were determined to be about  $7.17 \times 10^{-8} \Omega \text{ cm K}^{-1}$  and  $12.3 \times 10^{-5} \text{ K}^{-1}$ , respectively. It was found that the low TCR behavior was related to the magnetic transition and large lattice contraction. The origin of low TCR behavior was further analyzed based on the Labbé–Jardin tight-binding approximation model.

© 2010 Acta Materialia Inc. Published by Elsevier Ltd. All rights reserved.

**Keywords:** Low TCR; Magnetic transition; Lattice contraction;  $\text{Mn}_3\text{NiN}$

In recent years, many novel physical phenomena have been reported in the antiperovskite materials. Giant magnetoresistance in  $\text{Mn}_3\text{GaC}$  and superconductivity in  $\text{Ni}_3\text{MgC}$  are well known [1–3]. Very recently, the negative thermal expansion properties in  $\text{Mn}_3\text{Cu}(\text{Ge})\text{N}$  and large magnetostriction in  $\text{Mn}_3\text{CuN}$  were successively reported [4–6]. In our early work, the special magnetic, electronic transport property and lattice contraction in  $\text{Mn}_3\text{Zn}(\text{Ge})\text{N}$ ,  $\text{Mn}_3\text{Ga}(\text{Ge})\text{N}$  and  $\text{Mn}_3\text{Sn}(\text{Ge})\text{C}$  series compounds were also investigated [7–9].

In Ref. [10], Chi et al. reported the discovery of near-zero temperature coefficient of resistivity (TCR) in  $\text{Mn}_3\text{CuN}$ . The linear slope  $d\rho/dT$  and the TCR value are about  $1.42 \times 10^{-7} \Omega \text{ cm K}^{-1}$  and  $4.6 \times 10^{-5} \text{ K}^{-1}$ . The materials with near-zero TCR value can be used in a wide range of applications, such as resistor in high-precision electronic systems, temperature and flow sensors in automobiles and in thermo-electrical devices. Extensive work has been done to develop materials with low temperature coefficient of resistivity, such as new alloys based on  $\text{RuO}_2$  [11,12]. However, these materials possess the problem of oxidation on metal surface and bad adhesion due to structural strain. Compared with them, antiperovskite materials are very advantageous as they are isotropic and stable in air. Moreover, the near-zero TCR can be obtained in a pure form without forming composites.

However, only  $\text{Mn}_3\text{CuN}$  was reported in this series of materials. This inspires us to explore the possibility in other antiperovskite manganese nitrides.  $\text{Mn}_3\text{XN}$  compounds are strongly electron-correlated materials since the metal atoms on X sites provide itinerant electrons on the Fermi level. A systematic study based on almost 20 compounds and their solid solutions has shown that the character of their physical properties is controlled by the “electron density” around the metal X [13]. Thus, one of the promising candidates is Ni, which just lies on the left side of Cu in the Periodic Table.

The magnetic properties of  $\text{Mn}_3\text{NiN}$  have been described in the paper of Gomonaj [14]. Its primitive cell is cubic and contains three magnetic atoms. At low temperature, it has a triangular antiferromagnetic structure with the spins  $S_1$ ,  $S_2$ ,  $S_3$  of the manganese atoms along  $[1\ 1\ 0]$ ,  $[1\ 0\ 1]$  and  $[0\ 1\ 1]$ . With increasing temperature, a rotation of the magnetic moments occurs in the  $[1\ 1\ 1]$  plane through a total angle of  $90^\circ$ , and the magnetic moments are directed along  $[1\ 1\ 2]$ ,  $[1\ 2\ 1]$  and  $[2\ 1\ 1]$ , respectively, which reveal weak ferromagnetism. As the temperature is increased further, the compound shows a magnetic transition into the paramagnetic state. However, the electronic transport and thermal expansion behaviors have not been reported until now. In this letter, we reported the very low temperature coefficient of resistivity (L-TCR) of  $\text{Mn}_3\text{NiN}$  in a wide range from 250 K up to above room temperature. For understanding the essence of low TCR, the magnetic transport

\* Corresponding author. E-mail: [congwang@buaa.edu.cn](mailto:congwang@buaa.edu.cn)

and lattice properties were further investigated. A magnetic transition and a large isotropic lattice contraction phenomenon were observed with increasing temperature in this material, just before the L-TCR behavior. The relation among the low TCR, the magnetic transition and lattice contraction was discussed based on the electronic band structure of antiperovskite  $\text{Mn}_3\text{NiN}$ .

Polycrystalline sample  $\text{Mn}_3\text{NiN}$  was prepared by solid-state reaction using the powders of  $\text{Mn}_2\text{N}$  and Ni as the starting materials. Stoichiometric amounts of the starting materials were mixed, ground for 1 h and then pressed into pellets. The pellets were wrapped in a Ta foil and then sealed in a vacuumized ( $10^{-5}$  Pa) quartz tube. The quartz tube was sintered in a box furnace at  $800^\circ\text{C}$  for 48 h, and then cooled down to room temperature. The procedure was repeated three times until a pure phase was obtained.

X-ray diffraction (XRD) pattern of the resulting sample was obtained from an X'Pert PRO powder diffractometer. Structural characterization showed that the samples crystallize in the cubic system with  $Pm\bar{3}m$  space group. The sintered polycrystalline sample was cut into a bar shape ( $1 \times 2 \times 8$  mm) for the electrical resistivity measurement. The resistivity measurement was accomplished by standard four-probe technique from 120 to 330 K.  $\rho(T)$  curve from 120 to 350 K was measured with MPMS (Magnetic Property Measurement System), for which the temperature stability is  $\pm 0.5\%$  and temperature is accurate to less than  $\pm 1\%$ . For the lattice properties, variable temperature X-ray diffraction from 140 to 280 K was done on an X'Pert PRO powder diffractometer. The sample was heated to the desired temperature at a rate of  $10\text{ K min}^{-1}$  and held for 10 min. The XRD patterns at different temperatures were recorded, and then the lattice parameters were calculated by Powder X software [15]. Heat analysis was conducted using TAQ200 DSC in the temperature range from 180 to 480 K.

Figure 1a shows the curves of resistivity with temperature for  $\text{Mn}_3\text{NiN}$ . With increasing temperature, the resistivity continuously increases until about 240 K, exhibiting the metallic conduction behavior. Then, the resistivity data displays a small drop from 240 to 250 K. Above 250 K, the resistivity appears to be nearly

independent of temperature, which was readily noticed in the expanded view, as shown in the bottom-right inset of Figure 1a. Unfortunately, we could not measure the resistivity above 330 K due to the limit of the measuring temperature range. In the process of warming and cooling, the two resistivity curves almost coincide, shown in Figure 1a. This can be a great advantage as it implies that no microcrack and nitrogen releasing were produced during thermal cycling process.

We attempt to fit the  $\rho$ - $T$  curves according to any possible model. The result shows that the temperature dependence of resistivity below 240 K fits in the equation

$$\rho(\Omega, \text{cm}) = 0.1135 + 2.03 \times 10^{-6}T - 6.07 \times 10^{-10}T^2$$

From the equation, the coefficient of  $T$  is nearly four orders of magnitude greater than the coefficient of  $T^2$ , so the resistivity increases linearly with temperature. The curve above 250 K can be fitted into  $\rho(\Omega, \text{cm}) = 0.5389 + 7.17 \times 10^{-8}T$ . Then the value of  $d\rho/dT$  is determined as  $7.17 \times 10^{-8} \Omega \text{ cm K}^{-1}$  and the temperature coefficient of resistivity (TCR) value obtained from the equation of  $\rho_0^{-1}(d\rho/dT)$  is  $12.3 \times 10^{-5} \text{ K}^{-1}$  ( $250 \text{ K} < T < 330 \text{ K}$ ) while  $\rho_0$  is the resistivity at 250 K. As reported early, the slope  $d\rho/dT$  for  $\text{Mn}_3\text{CuN}$  was  $1.42 \times 10^{-7} \Omega \text{ cm K}^{-1}$  [10], which was nearly twice of  $\text{Mn}_3\text{NiN}$ . Therefore, the resistivity of  $\text{Mn}_3\text{NiN}$  was more independent of temperature.

This compound is a magnetic material. For analyzing the essence of the abnormal electronic transport properties, the magnetization was measured as a function of temperature at 50 Oe. As clearly seen in Figure 1b, the magnetic order undergoes a weak ferromagnetic to paramagnetic transition from 240 to 260 K with increasing temperature, which is consistent with the abrupt change of the resistivity and means that the low TCR behavior occurred in the paramagnetic state. Obviously, the change of spin order plays a crucial role for the low TCR behavior.

The temperature dependency of the resistivity for solids is susceptible to many influencing factors; no hard-and-fast rules are available. In  $\text{Mn}_3\text{NiN}$ , magnetic disorder and its effects on the electronic structure determine the changes of the local moments, which are in turn primarily responsible for the change of resistivity with temperature [16]. So the electronic band structure of  $\text{Mn}_3\text{NiN}$  compound holds the key to understand the abnormal electronic transport properties. According to the individual case of  $\text{Mn}_3\text{XN}$ , the structural and the magnetic phase transition take place at the same critical value of the temperature or not. Phase transition with a discontinuity in the variation of the volume alone has never been observed. A variation of the lattice volume induced by the magnetic transition also has a great influence on the electronic structure. Therefore, the temperature dependence of the lattice parameter was measured by variable temperature X-ray diffraction based on the magnetic transition.

All of the resultant XRD peaks at different temperatures were checked carefully. Only the shift of the peaks was found and no new peak appeared, i.e. the lattice kept cubic structure over the entire measured temperature range. The lattice parameters at different tempera-

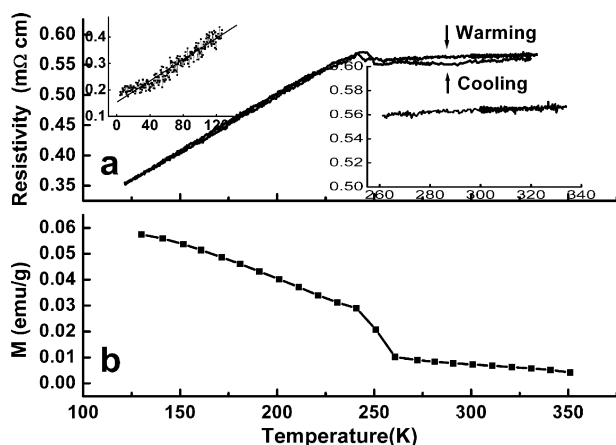


Figure 1. Temperature dependence of (a) the resistivity and (b) the magnetization for  $\text{Mn}_3\text{NiN}$ .

tures were obtained by indexing the XRD patterns. As shown in Figure 2, the lattice parameter first increases from 140 to 220 K and the linear thermal expansion coefficient is estimated to be  $\beta_1 = 3.47 \times 10^{-6} \text{ K}^{-1}$ .  $\beta_1$  is given by the following expression

$$\beta_1 = \left( \frac{1}{a_0} \right) \left( \frac{da}{dT} \right) = \left( \frac{1}{a_0} \right) \left( \frac{\Delta a}{\Delta T} \right)$$

where  $a_0$  is the lattice parameter at 273 K. Then, a big abrupt drop of the cubic lattice parameter ( $a$ ) takes place at around 220 K, i.e. an isotropic lattice contraction was observed. After 240 K, the lattice comes back to normal thermal expansion with increasing temperature. It is worth noting that this is consistent with the magnetic transition and the abrupt change of the resistivity. We repeated the measurement of XRD patterns at certain temperature and the same result was always remained, shown in Figure 2. This implied a good repeatability of this material. According to the thermodynamic view, a large lattice contraction is often accompanied by endothermal or exothermal phenomena. To further analyze the result, we carried out a calorimetric measurement. Upon heating, an obvious endothermic peak was observed around 242 K in the DSC curve, as shown in Figure 3. This is a sign of the first-order phase transition [17].

According to the Labbé–Jardin tight-binding approximation model, the electronic band structure of  $\text{Mn}_3\text{NiN}$  consists of a large conduction band overlapping a narrow band resulted from the strong hybridization between N-2p orbital and Mn-3d orbital [18]. In detail, the Fermi energy  $E_F$  lies inside the narrow d–p band and very close to the infinite singularity energy in the electronic density of states. So the abrupt change of the lattice parameter may result in the shift of the Fermi energy surface from one Brillouin zone to another one and has a major effect on the electronic structure [19].

From the band structure and the resistivity scale,  $\text{Mn}_3\text{NiN}$  can be viewed as semimetal. For narrow-band-gap semimetals, both the carrier mobility and the carrier density, or the number of the carriers, are temperature-dependent. However, the temperature dependence of the electrical conductivity is dominated by that of the latter, since the mobility changes only in a

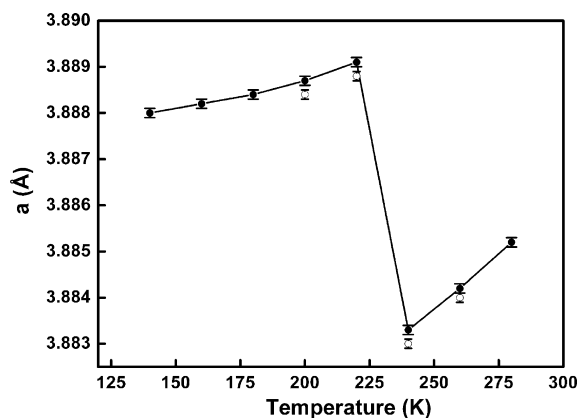


Figure 2. Temperature dependence of the lattice parameter (●) and the repeated result at certain temperature (○) for  $\text{Mn}_3\text{NiN}$  by variable temperature XRD.

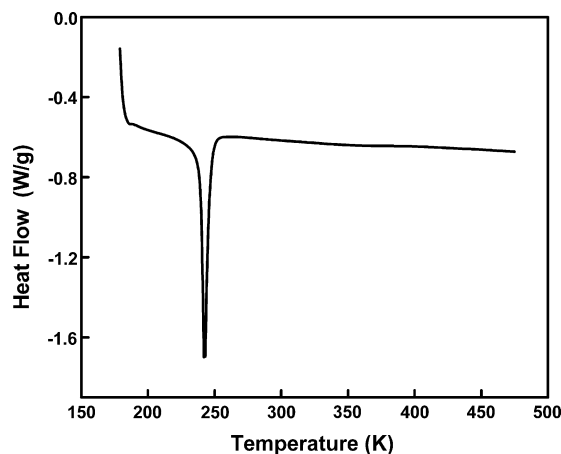


Figure 3. DSC curve from 180 to 480 K for  $\text{Mn}_3\text{NiN}$ .

mild way with the temperature while the number of carrier can be an exponential-like function of  $1/T$  [20]. Consequently, the resistivity increases linearly with temperature in the low temperature region. After the magnetic transition and the abrupt lattice contraction, the number of the carriers varies very slowly due to the change of the electronic structure or the band gap, which results in a delicate balance between the opposite changes of the number of carriers and the carrier mobility with temperature. Accordingly, the peculiar low TCR behavior occurs.

However, the low TCR behavior does not always exist in the series of  $\text{Mn}_3\text{XN}$  compounds. So far, only three compounds –  $\text{Mn}_3\text{NiN}$ ,  $\text{Mn}_3\text{AgN}$  (our unpublished work), and  $\text{Mn}_3\text{CuN}$  [10] – have such abnormal electronic transport properties. In  $\text{Mn}_3\text{XN}$ , the metal atoms on X sites offer itinerant electrons of the Fermi level. So the valence electron number of X atoms is a dominant factor for the electronic transport properties of  $\text{Mn}_3\text{XN}$  [13,16]. In the Periodic Table, Ag lies just under Cu and Ni on the left side of Cu. So we believe that the low TCR behavior must be also related to the outer electronic structure of the atom on X sites other than the electronic band structure of  $\text{Mn}_3\text{XN}$ . Theoretical calculation is in progress to elucidate the nature of low TCR.

In summary, a  $\text{Mn}_3\text{NiN}$  sample was prepared by solid-state reaction and its electronic transport, magnetic and lattice properties were studied. Excitedly, a very low temperature coefficient of resistivity was first found in  $\text{Mn}_3\text{NiN}$ . The  $d\rho/dT$  and TCR values for  $\text{Mn}_3\text{NiN}$  were determined as about  $7.17 \times 10^{-8} \text{ m}\Omega \text{ cm K}^{-1}$  and  $12.3 \times 10^{-5} \text{ K}^{-1}$  in the temperature range 250–330 K, respectively. A weak ferromagnetic to paramagnetic transition took place at around 240 K, just corresponding to the abrupt change of resistivity. Furthermore, there is a pronounced decrease of the lattice parameter around 240 K corresponding to the magnetic transition. The magnetic transition and large lattice contraction, which have a great influence on the electronic structure, hold the key to understand the occurring of the peculiar low TCR. A delicate balance between the opposite changes of the number of carriers and of the carrier mobility with temperature was the phenomenological cause. Although the origin of low TCR needs to be

confirmed by further exploration, the current result will bring some significance to solid-state physics. It will inspire the search for similar materials and promote an in-depth investigation of the detailed operating mechanisms.

This work was financially supported by National Natural Science Foundation of China (NSFC) (No. 50772008) Key Laboratory of Micro-nano Measurement, Manipulation and Physics (Ministry of Education) and Metastable Materials Science and Technology State Key Laboratory of Yanshan University.

- [1] K. Kamishima, T. Goto, H. Nakagawa, N. Miura, M. Ohashi, N. Mori, T. Sasaki, T. Kanomata, *Phys. Rev. B* 63 (2000) 024426.
- [2] T. He, Q. Huang, A.P. Ramirez, Y. Wang, K.A. Regan, N. Rogado, M.A. Hayward, M.K. Haas, J.S. Slusky, K. Inumara, H.W. Zandbergen, N.P. Ong, R.J. Cava, *Nature* 411 (2001) 54.
- [3] H. Rosner, R. Weht, M.D. Johannes, W.E. Pickett, E. Tosatti, *Phys. Rev. Lett.* 88 (2002) 027001.
- [4] K. Takenaka, H. Takagi, *Appl. Phys. Lett.* 87 (2005) 261902.
- [5] S. Iikubo, K. Kodama, K. Takenaka, H. Takagi, S. Shamoto, *Phys. Rev. B* 77 (2008) 020409(R).
- [6] K. Asano, K. Koyama, K. Takenaka, *Appl. Phys. Lett.* 92 (2008) 161909.
- [7] Y. Sun, C. Wang, Y.C. Wen, K.G. Zhu, J.T. Zhao, *Appl. Phys. Lett.* 91 (2007) 231913.
- [8] Y. Sun, C. Wang, Y.C. Wen, *Mater. Sci. Forum* 561–565 (2007) 557.
- [9] Y.W. Wen, C. Wang, Y. Sun, *Solid State Commun.* 149 (2009) 1519.
- [10] E.O. Chi, W.S. Kim, N.H. Hur, *Solid State Commun.* 120 (2001) 307.
- [11] Y.T. Kim, *Appl. Phys. Lett.* 70 (2) (1997) 209.
- [12] B. Fu, L. Gao, *Scr. Mater.* 55 (2006) 521.
- [13] D. Fruchart, E.F. Bertaut, *J. Phys. Soc. Jpn.* 44 (3) (1978) 781–791.
- [14] E.V. Gomonaj, *Phase Transitions* 18 (1–2) (1989) 93.
- [15] C. Dong, *J. Appl. Cryst.* 32 (1999) 838.
- [16] K. Motizuki, H. Nagai, *J. Phys. C: Solid State Phys.* 21 (1988) 5251–5258.
- [17] J. García, R. Navarro, J. Bartolomé, D. González, D. Fruchart, *J. Chem. Thermodyn.* 15–18 (1980) 1155–1156.
- [18] J.P. Jardin, J. Labbe, *J. solid State Chem.* 46 (1983) 275–293.
- [19] Y.B. Li, W.F. Li, W.J. Feng, Y.Q. Zhang, Z.D. Zhang, *Phys. Rev. B* 72 (2005) 024411.
- [20] A.L. Ji, C.R. Li, Z.X. Cao, *Appl. Phys. Lett.* 89 (2006) 252120.